

## Investigation of electron-irradiated zinc by diffuse x-ray scattering. II. Interstitial clustering during thermal annealing

B. Schönfeld and P. Ehrhart

*Institut für Festkörperforschung der Kernforschungsanlage Jülich, D-5170 Jülich, Germany*

(Received 22 September 1978)

The diffuse scattering intensity near Bragg reflections and the electrical-resistivity change following electron irradiation of zinc single crystals at 4.5 K were investigated during an isochronal annealing program. The initial Frenkel defect concentration varied between 18 and 120 ppm. At the end of recovery stage I (at 20 K) small interstitial agglomerates are formed. For the higher irradiation doses, cluster growth continues during recovery stage II up to an effective cluster size of  $\langle N \rangle \approx 10$  interstitials per agglomerate, but is strongly suppressed for the lowest initial defect concentration. The results are understood within the framework of the one-interstitial recovery model.

### I. INTRODUCTION

In Paper I it was shown that  $e^-$  irradiation of zinc at low temperature produces a statistical distribution of single interstitials and vacancies.<sup>1</sup> The characteristic properties observed for the single interstitial were a large relaxation volume  $\Delta V^{i,rel} = 3.6$  atomic volumes and a strong anisotropy of the long-range part of its displacement field with a large displacement in the  $c$  direction and a small displacement in the basal plane. This anisotropy led to an anisotropic diffuse-scattering intensity with a high intensity in the  $[00.1]$  direction close to an  $(00.h)$  reflection. For this special direction the diffuse-scattering cross section  $S_H$  can be written (for details see Paper I)

$$S_H = C |F_{\vec{K}}|^2 \left(\frac{h}{q}\right)^2 \frac{1}{V_c^2} \left(\frac{P_{33}}{c_{33}}\right)^2, \quad (1)$$

where  $\vec{q} = \vec{K} - \vec{h}$  is the distance of the scattering vector  $\vec{K}$  from the nearest reciprocal-lattice vector  $\vec{h}$ ,  $C$  is the total concentration of interstitial atoms,  $F_{\vec{K}}$  is the structure factor of the hexagonal lattice,  $V_c$  is the volume of the unit cell, and  $c_{33}$  and  $P_{33}$  are the components of the elastic constant and dipole-force tensors, respectively.

During thermal annealing interstitials become mobile and form agglomerates. Because of the quadratic dependence of  $S_H$  on  $P_{ij}$  [or the relaxation volume  $\Delta V^{i,rel}$ , which is directly connected with  $P_{33}$  according to Eq. (7) of Paper I] the Huang-scattering cross section is very sensitive to this agglomeration. Assuming linear superposition of the individual defect-displacement fields upon clustering,  $S_H$  increases by a factor  $N$  if the interstitials form clusters of  $N$  interstitials per cluster (since  $C_{cl} = C/N$  and  $P_{33}^{cl} = NP_{33}^i$ ). Mobile

interstitials will not only agglomerate but also recombine with vacancies. This change in the interstitial concentration can be considered by normalizing  $S_H$  to the resistivity change  $\Delta\rho$ , which generally is a good measure for the total defect concentration. If the assumption of a linear superposition of the defect-displacement fields is not valid, we must consider the change of  $\Delta V^{i,rel}$  to the relaxation volume of an interstitial in a cluster  $\Delta V_{cl}^{i,rel}$ . The effective cluster size  $\langle N \rangle$  as a function of the annealing temperature  $T$  becomes

$$\langle N \rangle = \frac{S_H^{cl}(T)}{S_H^i(6\text{ K})} \frac{\Delta\rho(6\text{ K})}{\Delta\rho(T)} \left(\frac{\Delta V^{i,rel}}{\Delta V_{cl}^{i,rel}}\right)^2. \quad (2)$$

The quadratic dependence on  $\Delta V^{i,rel}$  is consistent with Ref. 2, as in the case of Al an exact proportionality between  $\Delta\rho$  and  $\Delta a/a$  is established; this allows a measure of the defect concentration by the lattice-parameter change [ $C = 3(\Delta a/a)/(\Delta V^{i,rel}/\Omega)$ ]. Therefore for a cubic crystal we reduce the quadratic dependence of Eq. (2) on  $\Delta V^{i,rel}$  to a linear one.

If there is a broad distribution of cluster sizes,  $\langle N \rangle$  is an effective cluster size, where the larger clusters carry a higher weighting in  $S_H$ . For the small cluster sizes observed in the present investigation the size distribution is not very important, and the effective sizes should also very well represent the average size of the agglomerates.

With increasing cluster size, the Huang scattering is restricted to a region of smaller  $q$  values around the Bragg reflection. The transition between the  $q^{-2}$  dependence of the Huang scattering  $S_H$  and the  $q^{-4}$  dependence, that is observed at larger  $q$  values is characterized by a critical value  $q_{cr}$ , which may be associated with a critical radius  $R_0$  ( $q_{cr} \approx 1/R_0$ ).<sup>1</sup> For low reflection orders  $R_0$  roughly represents the cluster radius  $R_{cl}$ . For

larger  $q$  values, the diffuse scattering images the strongly distorted region in the vicinity of the clusters which is described by the asymptotic or Stokes-Wilson scattering cross section

$$S_{SW} = 147 C_{cl} |F_{\vec{K}}|^2 \left| \frac{\Delta V^{cl,rel}}{4\pi\gamma} \right| \frac{h}{q^4 V_c^2}, \quad (3)$$

where  $\Delta V^{cl,rel}$  is the relaxation volume for a cluster. This expression is valid for isotropic defects in an isotropic matrix and the numerical value 147 holds for  $\vec{q}$  parallel  $\vec{h}$ . In contrast to  $S_H$ ,  $S_{SW}$  depends only linearly on the relaxation volume and therefore is independent of the cluster size under the assumptions made above ( $C_{cl} = C/N$  and  $\Delta V^{cl,rel} = N\Delta V^{i,rel}$ ).

In Sec. II we present the experimental results obtained after an isochronal annealing program of  $e^-$ -irradiated zinc by measuring the diffuse x-ray scattering intensity and the change of the electrical resistivity. The determination of the size of interstitial clusters based on Eqs. (1)–(3) is discussed in detail. In Sec. III the results of the annealing experiments are discussed and compared to the literature.

## II. EXPERIMENTAL

After electron irradiation at 4.5 K and the initial measurements at about 6 K (described in Paper I) the Zn single crystals were annealed in an isochronal annealing program with 20-min holding times. The diffuse-scattering intensity close to (00.4), (00.6), and (11.0) reflections was measured at 6 K. The corresponding resistivity change was measured with the sample in liquid He. Absolute temperatures were accurate to 2 K up to about 50 K and to 5 K at higher temperatures.

### A. Observation of interstitial clustering

As an example, the recovery behavior of the diffuse scattering at the (00.4) reflection in the [00.1] direction of sample Zn 4 (for a description of the samples see Paper I) is shown in Fig. 1. For the (00.6) reflection similar results were obtained. With increasing recovery temperature (up to 105 K) the intensity close to the Bragg reflection does not change significantly, but the region of the Huang scattering is restricted to smaller  $q$  values. At larger  $q$  values we observe a steeper decrease, that can be described by a  $q^{-4}$  dependence as is expected for scattering by clusters. A detailed annealing program is given in Fig. 2(a). The Huang scattering and the electrical-resistivity change are normalized to their initial values at 6 K. For the Huang scattering the average  $S_H q^2$  is taken, that is a constant according to Eq. (1). As  $S_H$  is restricted to small values of  $q$  at higher temperatures the errors

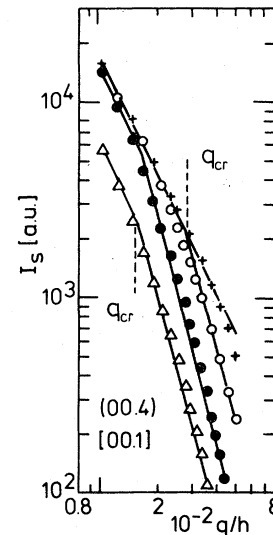


FIG. 1. Symmetrical part of the diffuse-scattering intensity  $I_s$  at  $\vec{h}$ : (00.4),  $\vec{q}$ : [00.1] of Zn 4 [ $\Delta\rho$  (4.5 K) = 215 n $\Omega$  cm]: after irradiation at 6 K (+), after recovery at 60 K (O), 105 K (●), and 130 K (Δ).

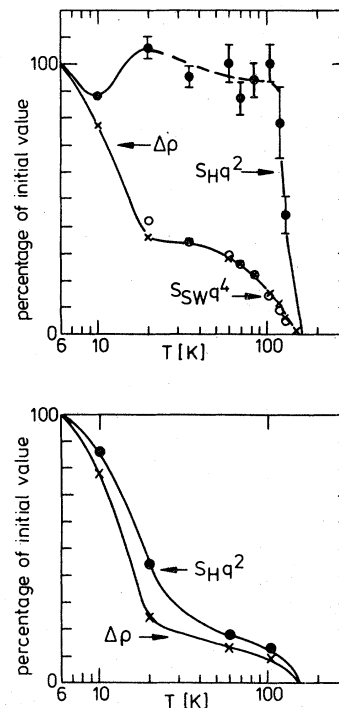


FIG. 2. Recovery behavior of the diffuse-scattering intensity in the Huang region (●)  $S_H q^2(T)/S_H q^2(6\text{ K})$  and in the Stokes-Wilson region (O)  $[S_{SW} q^4(T)/S_{SW} q^4(35\text{ K})] \times \Delta\rho(35\text{ K})$ , and of the electrical-resistivity change (X)  $\Delta\rho(T)/\Delta\rho(6\text{ K})$ : (a) of Zn 4 [ $\Delta\rho$  (4.5 K) = 215 n $\Omega$  cm]; (b) of Zn 3 [ $\Delta\rho$  (4.5 K) = 32 n $\Omega$  cm].

TABLE I. Dependence of the effective cluster size  $\langle N \rangle$  on the initial-defect concentration  $C$  (6 K) as determined at (00.*h*) reflections.

Sample $C$ (6 K) (ppm)	Zn 3 18	Zn 2 68	Zn 1 72	Zn 6 88	Zn 4 120
$\langle N \rangle$ (20 K), end of stage I	1-2	2-3	2-3	2-3	3 3 <sup>a</sup>
$\langle N \rangle$ (105 K), end of stage II	1-2	4-6	5-8	5-8	5-8
$\langle N \rangle$ (130 K), stage III		5-8 <sup>a</sup>	7-10 <sup>a</sup>	7-10 <sup>a</sup>	7-10 <sup>a</sup>
				6-9	6-9

<sup>a</sup>Determined according to Eq. (5).

get larger. The error bars were estimated from the variations between the results for the (00.4) and (00.6) reflections. According to Eq. (2) the ratio of the two curves in Fig. 2(a) at equal annealing temperatures yields the effective cluster sizes  $\langle N \rangle$ .

A similar recovery behavior was observed with Zn 1, 2, and 6. Results for the effective cluster size  $\langle N \rangle$  are summarized in Table I. We find that  $\langle N \rangle$  increases with increasing initial-defect concentration  $C$  (6 K). With Zn 3, the sample with the smallest irradiation dose,  $\Delta\rho$  and the Huang scattering exhibit nearly parallel recovery: the formation of clusters is, therefore, strongly suppressed [see Fig. 2(b)]. With an effective cluster size of one or two interstitials, di-interstitials and perhaps trapped single interstitials dominate the size distribution.

#### B. Discussion of the cluster size

The determination of  $\langle N \rangle$  from the Huang scattering [Eq. (2)] is based on the assumption that the electrical resistivity  $\Delta\rho$  is a reliable measure of the total interstitial concentration during clustering. Of more concern is the assumption of the linear-superposition model ( $\Delta V^{i,rel} = \Delta V_{cl}^{i,rel}$ ). This assumption is especially critical for zinc, where  $(\Delta V/\Omega)^{i,rel} = 3.6$  for the single interstitial is much larger than the limiting value per interstitial in an infinite dislocation loop with  $(\Delta V/\Omega)_{cl}^{i,rel} \approx 1$ . Therefore, the consistency of the relaxation volume as determined by two independent methods and also that of the effective cluster size is checked in the following.

First, the relaxation volume is given by measurements of the lattice-parameter change. If we assume that  $\rho_F$  does not vary during the formation of small agglomerates in stage I, a change of the ratio  $\eta = (\Delta c/c)/\Delta\rho$  during annealing directly yields the change of the relaxation volume (of interstitial and vacancy). Following irradiation we had obtained an average value  $\eta = (3.05 \pm 0.3) \times 10^3 (\Omega \text{ cm})^{-1}$  at 6 K (see Paper I). At about 12 K

we obtained  $(2.85 \pm 0.3) \times 10^3 (\Omega \text{ cm})^{-1}$  for Zn 5 and at 20 K  $(2.55 \pm 0.5) \times 10^3 (\Omega \text{ cm})^{-1}$  for Zn 4. At higher annealing temperatures  $\Delta c/c$  could not be measured with sufficient accuracy because of the small total defect concentration remaining. Thus up to 20 K we observe a change of about 15%, that is still within the measuring errors. Within the experimental accuracy the linear-superposition model used in Eq. (2) is therefore a reasonable approximation up to 20 K.

Second, at temperatures above 20 K, where interstitial clusters are observed, we can get information about the relaxation volume from the Stokes-Wilson scattering. Considering the elastic anisotropy of Zn and the anisotropy of the interstitial clusters, an estimate of  $S_{sw}$  can be given according to Eq. (3). The elastic anisotropy of Zn is considered in the determination of the Eshelby constant  $\gamma = 3(1-\nu)/(1+\nu)$  by calculating an "isotropically averaged" Poisson ratio  $\nu$ .<sup>3</sup> With  $\nu = 0.234$  we obtain  $\gamma = 1.86$  at 6 K. In contrast to fcc metals,<sup>4,5</sup> for hcp Zn the orientation of the clusters on the basal plane must be considered. In order to obtain an average we take one-third of the scattering intensity (measured in the preferred [00.1] direction at the (00.4) reflection). As a mean value of all samples (except Zn 3) we get  $(\Delta V/\Omega)^{i,rel} = 4.9 \pm 1.9$  at 35 K (in this evaluation the concentration  $C$  was determined from  $\Delta\rho$  assuming that  $\rho_F = 15.3 \mu\Omega \text{ cm/at.}\%$  has not changed during clustering). The measurements at 35 K were chosen, because at 20 K there are still some variations (within 20%) indicating that not all interstitials have agglomerated in clusters large enough to give the full contribution to the Stokes-Wilson scattering [see Fig. 2(a)]. The high value of  $\Delta V^{i,rel}$  obtained from the Stokes-Wilson scattering is in agreement with the value observed for single interstitials from Huang scattering (Paper I); this suggests that not much relaxation had occurred up to 35 K.

Although the absolute value of  $(\Delta V/\Omega)^{i,rel}$  de-

terminated from  $S_{sw}$  may contain a large systematic error, a change of  $(\Delta V/\Omega)^{i,rel}$  during annealing can be reliably detected by comparing the annealing of the defect concentration  $C$  (or  $\Delta\rho$ ) with the annealing of  $S_{sw}$ . For this comparison  $S_{sw}$  and  $\Delta\rho$  have been normalized at 35 K. From Fig. 2(a) we see a similar recovery behavior of  $\Delta\rho$  and  $S_{sw}$  from 35 to 85 K. At the end of stage II and in stage III,  $S_{sw}$  tends to a faster recovery (e.g., by 15% at 105 K). This behavior was confirmed with the other samples. With the assumption that all defects are in clusters and  $\Delta\rho$  measures the total defect concentration  $C$ , the faster recovery above 85 K implies that the relaxation volume decreases during isochronal annealing at the end of stage II. Including this relaxation yields an increase of the cluster size  $\langle N \rangle$  of Table I (e.g., by 30% for Zn 4 at 105 K, which is within the quoted uncertainties).

Finally, the effective cluster size is also obtained by the combination of  $S_H$  and  $S_{sw}$ . This procedure is equivalent to that in Paper I if we replace the lattice parameter change  $\Delta c/c$  by  $S_{sw}$ . This evaluation can be simply reduced to the determination of  $q_{cr}$ , where the slope of the intensity changes from  $-2$  to  $-4$  (Fig. 1). At this point, determined by graphical extrapolation,  $S_H$  [Eq. (1)] and  $S_{sw}$  [Eq. (3)] are equal. This procedure yields

$$q_{cr} = \left( 3 \frac{\Delta V^{cl,rel}}{4\pi\gamma} \frac{147}{h} \right)^{1/2} \frac{C_{33}}{P_{33}^{cl}}. \quad (4)$$

The factor of 3 considers the preferred orientation of the clusters as explained above. With the ratio  $P_{33}/P_{11} = 2.5$  and Eq. (7) of Paper I, which gives the relation between  $\Delta V^{rel}$  and  $P_{ij}$  we get  $q_{cr} \sim (\Delta V^{cl,rel})^{-1/2}$ . By using the linear-superposition model ( $\Delta V^{cl,rel} = N\Delta V^{i,rel}$ ) we may determine  $\langle N \rangle$  from the experimental value of  $q_{cr}$ :

$$\langle N \rangle = 0.0566 \text{ \AA}^{-2} / q_{cr}^2. \quad (5)$$

As shown in Table I the value of  $\langle N \rangle$  determined by this method agrees with those calculated from Huang scattering within the temperature range from 35 to 90 K; at 105 K however, it is about 20%–30% higher. This is consistent with a relaxation volume change of about 15% as determined from  $S_{sw}$ .

In this evaluation several different approximations were used. By using Eq. (4) we eliminate the total defect concentration and are therefore independent of the assumption on the resistivity<sup>5</sup> (see also Ref. 4 for a review on the determination of cluster sizes). In addition, the relaxation volume enters only linearly and is therefore a

less serious error source. The main error of this method is the possible systematic error of Eq. (3) discussed above and the uncertainty in the determination of  $q_{cr}$ . This determination is not precise, because there is no exact  $q^{-4}$  dependence. In fact, the " $q^{-4}$  region" has some structure. Such deviations from a  $q^{-4}$  dependence can be seen in Fig. 1, although the curves shown there are the average of the measurements on opposite sides of the Bragg reflection.

### C. Symmetry of the clusters

The diffuse scattering at  $(00.h)$  reflections discussed above images the displacements in the  $c$  direction ( $S_H \sim CP_{33}^2$ ). The displacements in the basal plane are imaged by measurements at  $(hh.0)$  or  $(h0.0)$  reflections with  $\vec{q}$  in the direction of the reciprocal-lattice vector ( $S_H \sim CP_{11}^2$ ; see Paper I). The recovery behavior of the scattering intensity at the  $(11.0)$  reflection is shown in Fig. 3. As in the measurement immediately following irradiation (Paper I) the intensities are much lower than at  $(00.h)$  reflections. After recovery at 10 K the intensity is very similar to that observed directly after the irradiation; i.e., for larger values of  $q$  the decrease of the intensity is still slower than  $q^{-2}$ . However this slow decrease disappears at 20 K thus indicating a change of the defect structure. This conclusion is supported by the result that at this temperature the Huang-scattering intensity per defect (as obtained by normalizing with  $\Delta\rho$ ) increases. At higher recovery temperatures a

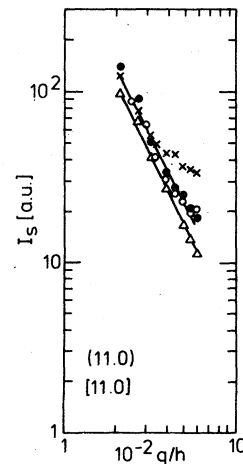


FIG. 3. Symmetrical part of the diffuse-scattering intensity  $I_S$  at  $h$ :  $(11.0)$ ,  $q$ :  $[11.0]$  of Zn 6 [ $\Delta\rho$  (4.5 K) = 153 n $\Omega$  cm]; after recovery at 10 K ( $\times$ ), 20 K ( $\circ$ ), 105 K ( $\bullet$ ), and 130 ( $\Delta$ ).

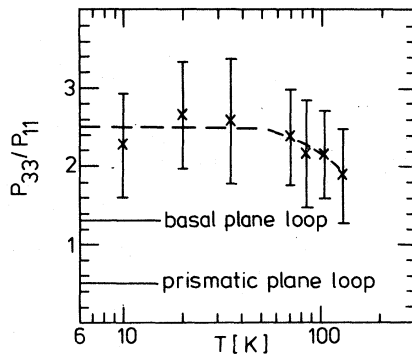


FIG. 4. Recovery behavior of the symmetry parameter  $P_{33}/P_{11}$  of Zn 6 in comparison with  $P_{33}/P_{11}$  for pure prismatic loops on basal and prismatic planes.

$q^{-2}$  rather than a  $q^{-4}$  behavior is found within a measuring range that exhibits a  $q^{-4}$  dependence for the (00.4) reflection (see Fig. 1). This shift of  $q_{cr}$  to larger  $q$  values than at the (00.4) reflection that has a comparable length of  $h$ , can be understood from Eq. (4) as  $P_{33}$  has to be replaced by  $P_{11}$  and the  $c_{ij}$  similarly (see Paper I). Thus this different behavior at the (11.0) reflection indicates that the displacements in the basal plane (determined by  $P_{ij}$  and  $c_{ij}$ ) are still smaller than in the  $c$  direction.

By dividing the Huang intensities at (00. $h$ ) and ( $hh$ .0) reflections we obtain the concentration-independent ratio  $P_{33}^2/P_{11}^2$  that characterizes the symmetry of the defect. Figure 4 shows the annealing behavior of this parameter. It has the value of 2.5 for the  $c$ -split  $H_c$  (Paper I) and tends to lower values with increasing  $\langle N \rangle$  at the end of stage II. The main uncertainty in this result is caused by the (11.0) reflection, where we have a high statistical error.

The experimental value of  $P_{33}/P_{11}$  can be compared with theoretical values for different loop types, as given by Trinkaus<sup>3</sup> from elastic continuum theory: for pure prismatic-dislocation loops on basal and prismatic planes,  $P_{33}/P_{11}$  is equal to  $c_{33}/c_{13} = 1.27$  and  $2c_{13}/(c_{11} + c_{12}) = 0.51$ , respectively (data for zinc). With  $P_{33}/P_{11} = 2.1 \pm 0.6$  at the end of recovery stage II the theoretical value for loops on the basal plane is closer to the experiment. This is consistent with the general observation that loops condense on close packed planes. For Zn with  $c/a > \sqrt{3}$  these are the basal planes (for  $c/a < \sqrt{3}$ , loops on prismatic planes would be expected<sup>6</sup>). On the other hand the ratio  $P_{33}/P_{11}$  still remains between that for a single interstitial and a dislocation loop indicating that these small clusters are not well described by dislocation loops.

### III. DISCUSSION OF THE ANNEALING BEHAVIOR

In the discussion of the annealing behavior of electron-irradiated zinc we may roughly distinguish between four regions [see Fig. 2(a)].

(a) Between 6 and 10 K, both the electrical-resistivity change and Huang scattering decrease. This means that the recovery results primarily from the recombination of close Frenkel pairs (subpeaks  $I_B$  at 7 K and  $I_C$  at 9 K). [At present there is no well-established picture of the annealing spectrum of Zn. As the irradiation conditions of Vandenborre *et al.*<sup>7</sup> were most similar to ours, we will use their nomenclature, although there is evidence that more recovery substages (corresponding to different close-pair configurations)<sup>8,9</sup> are present in stage I after  $e^-$  irradiation than given by Ref. 7]. The remaining defects are unchanged. The somewhat lower recovery rate of the diffuse-scattering intensity compared with  $\Delta\rho$  indicates that the first small agglomerates are formed.

(b) From 10 K to the end of stage I at 20 K,  $\Delta\rho$  strongly decreases, whereas the Huang scattering increases, indicating that interstitial clustering is occurring. Independent of the question whether a dose-dependent substage  $I_E$  (i.e., free migration) is observed in Zn,<sup>7-9</sup> this observation directly demonstrates the long-range migration of interstitials in stage I. However, from the present results it cannot be discriminated, whether the migration of the  $c$ -split interstitial is three-dimensional or whether it is one-dimensional as claimed by Seeger and Gösele<sup>10</sup> for Cd.

(c) In stage II (substages IIA at 20 K–60 K and IIB at 60 K–105 K) the clusters continue to grow slowly to an effective cluster size  $\langle N \rangle \approx 8$  interstitials per cluster. The strong suppression of the interstitial clustering for the lowest irradiation dose [Fig. 2(b)] seems reasonable: first, at low dose we have a higher percentage of correlated Frenkel pair annealing and therefore less interstitial interaction. This is in accordance with the more pronounced recovery of  $\Delta\rho$  within stage I of 76% with Zn 3 compared to 62% with Zn 4. Second, for Zn 3, the defect concentration after stage I (2–4 ppm) is comparable with the concentration of impurities, which might serve as traps thus suppressing interstitial clustering. The different annealing behavior of samples with low ( $\Delta\rho = 32$  n $\Omega$  cm) and high ( $\Delta\rho = 215$  n $\Omega$  cm) defect concentrations can be compared with the annealing data of the electrical resistivity of Vandenborre *et al.*<sup>7</sup> In the same concentration range they observed an annealing peak at the end of stage II (at 85 K) which increased with initial-defect concentration. Therefore we attribute this substage tentatively to the migration of small-inter-

stitial agglomerates that are not built up at low-defect concentrations.

(d) In stage III (105–160 K) both Huang scattering and  $\Delta\rho$  decrease. Within the accuracy of measurements we obtain full recovery at 160 K. This can be understood if vacancies become mobile in stage III, and dissolve the interstitial clusters by recombination reactions, as it is predicted by the one-interstitial recovery model,<sup>11</sup> that attributes annealing stage I to the interstitial and stage III to the vacancy migration.

The annealing behavior of Zn appears very similar to that of the fcc metal Al. Under similar irradiation conditions the formation of small interstitial agglomerates was observed in Al at the end of stage I with a slow and steady growth of the agglomerates throughout stage II.<sup>2,12</sup> Although there are no model calculations for small interstitial agglomerates in hcp metals we expect that the concepts developed for the cluster growth in fcc metals can also be applied to Zn. In agreement with model calculations<sup>13</sup> and the experimental investigations of diffuse x-ray scattering<sup>2,12</sup> and mechanical-relaxation experiments,<sup>14</sup> the small interstitial agglomerates in fcc metals are characterized by a high binding energy and a low activation energy of motion. Thus cluster growth can be explained by the motion and coalescence of existing clusters (assisted by their mutual strain field). This model of cluster growth is supported by the behavior of the  $q^{-4}$ -scattering intensity. The, at first, parallel and, at higher temperatures, even faster annealing of  $S_{sw}$  compared with  $\Delta\rho$  indicates that, in Zn as in Al and Cu,<sup>5</sup> the majority of interstitials are present in the form of clusters already at the beginning of stage II. Second, we observe between 35 K and 105 K [Fig. 2(a)] a decrease of  $S_{sw}$  by more than 50%. This demonstrates that interstitials, that

have already been part of a cluster, recombine with vacancies. Because of the high binding energies of small interstitial agglomerates a dissolution of small clusters and growth of the larger ones seems to be unlikely. Therefore, the loss of these interstitials should be explained by recombinations with vacancies that are absorbed on the path of the interstitial agglomerates.

#### IV. SUMMARY

Zn single crystals electron irradiated at low temperature were investigated during an isochronal annealing program. At the end of recovery stage I small interstitial agglomerates were found which grew during recovery stage II depending on the initial-defect concentration. A consistent picture of small cluster sizes (up to ten interstitials per cluster) determined by different evaluation techniques was seen. The symmetry of these small agglomerates remains between that for a single interstitial and a dislocation loop in the basal plane. Consistent with the small size of the agglomerates, the symmetry parameter indicates that these agglomerates are not well described by dislocation loops. The agglomerates anneal completely during stage III. This can be straightforwardly explained in the one-interstitial recovery model where the vacancies become mobile and dissolve the interstitial clusters.

#### ACKNOWLEDGMENTS

The authors want to thank Dr. H. Trinkaus for many discussions and for making his unpublished results available to us. Last, but not least, they also thank Professor W. Schilling and Dr. J. B. Roberto for carefully reading the manuscript.

<sup>1</sup>P. Ehrhart and B. Schönfeld, preceding paper, Phys. Rev. B **19**, 3896 (1979).

<sup>2</sup>J. B. Roberto, B. Schönfeld, and P. Ehrhart, Phys. Rev. B **18**, 2591 (1978).

<sup>3</sup>H. Trinkaus (private communication).

<sup>4</sup>B. C. Larson, in *Fundamental Aspects of Radiation Damage in Metals*, edited by M. T. Robinson and F. W. Young, Jr. (U. S. GPO, Washington, D.C., 1975), p. 820.

<sup>5</sup>P. Ehrhart and U. Schlagheck, J. Phys. F **4**, 1589 (1974).

<sup>6</sup>M. Wilkens, in Ref. 4, p. 470.

<sup>7</sup>H. Vandenborre, J. Nihoul, and L. Stals, Cryst. Lattice Defects **5**, 89 (1974).

<sup>8</sup>S. Myhra, Phys. Status Solidi A **43**, 579 (1977).

<sup>9</sup>J. Roggen, J. Nihoul, J. Cornelis, and L. Stals, J. Nucl. Mater. **69–70**, 700 (1978).

<sup>10</sup>A. Seeger and U. Gösele, Radiat. Eff. **24**, 123 (1975).

<sup>11</sup>W. Schilling, P. Ehrhart, and K. Sonnenberg, in Ref. 4, p. 268.

<sup>12</sup>P. Ehrhart and W. Schilling, Phys. Rev. B **8**, 2604 (1973).

<sup>13</sup>H. R. Schober, J. Phys. F **7**, 1127 (1977).

<sup>14</sup>K. H. Robrock, L. E. Rehn, V. Spiric, and W. Schilling, Phys. Rev. B **15**, 680 (1977); V. Spiric, L. E. Rehn, K. H. Robrock, and W. Schilling, *ibid.* **15**, 672 (1977).